Int. J. Electrochem. Sci., 8 **(2013)** 2842 - 2848

International Journal of
ELECTROCHEMICAL
SCIENCE
www.electrochemsci.org

Short Communication

Synthesize of Graphene-$LiFePO_4$ Composite Porous Microsphere with the Enhanced Rate Performance

Yuan Ma, Xianlei Li, Shifu Sun, Xiaopeng Hao[*]*, Yongzhong Wu*[*]

State Key Lab of Crystal Materials, Shandong University, Jinan, 250100, Shandong, P. R. China
[*]E-mail: xphao@sdu.edu.cn; wuyz@sdu.edu.cn

Received: 27 November 2012 / *Accepted:* 15 December 2012 / *Published:* 1 February 2013

Graphene materials have been proved an advantage for application in energy storage due to the superior electrical conductivities and high surface area. The structure of porous microsphere is reported as an effective way to achieve high energy density and high power density for $LiFePO_4$. It is worthwhile to examine the influence of the combination of graphene and porous structure of $LiFePO_4$ on the performance of Li-ion battery. To this end, graphene-$LiFePO_4$ (G-LFP) composite porous microspheres are successfully synthesized using the as-prepared graphene oxide-Li_3PO_4 as sacrificial template. The microspheres showed a uniform morphology that 2 μm $LiFePO_4$ microspheres are wrapped by graphene nanosheets. And the microspheres exhibit the hierarchical structures assembled by nanoparticles. The cathodes made from G-LFP deliver excellent rate performance that hold 72% of the initial capacity at 10 C. The enhanced performance is attributed to the high conductivity of graphene network in composite and its porous structure in favor of lithium ion diffusion.

Keywords: graphene-lithium iron phosphate; porous microsphere; graphene oxide- lithium phosphate; rate performance.

1. INTRODUCTION

Lithium iron phosphate is expected as a new generation of Li-ion batteries because of its high safety, low cost and low toxicity, etc. [1,2]. However, the low intrinsic electronic and ionic conductivities limit its development and application [3,4]. Coating the $LiFePO_4$ particles with carbon layer [5] and decreasing the distance of Li-ion diffusion [6] are effective ways to overcome these drawbacks.

Recently, graphene has found a variety of application in energy conversion and storage devices [7], due to the excellent properties such as high electronic conductivity, structural flexibility, stability, mechanical strength and surface area [8]. Up to date, several methods have been used to prepare graphene-$LiFePO_4$ (G-LFP) composites, such as hydrothermal method [9,10], sol-gel method [11],

solid-state method [12], co-precipitation method [13]. The morphologies of the reported G-LFP mostly are nanoparticles that go against the development of the high tap density. And in terms of the rate performance, there is a room for improvement.

As for decreasing the distance of Li-ion diffusion, a 3D nanoporous micron-sized sphere is considered as an optimal structure for $LiFePO_4$, which could realize high power capability without compromising the packing density and facilitate the fast and efficient transport of ion and charge [14]. Yang et al. prepare G-LFP porous composite using a sol-gel method [11]. However, oversize hole fail to achieve the advantage of the high tap density of porous structure, and nonuniform distribution of graphene did not show significantly improve on electrochemical performance.

Herein we present a novel synthesis of G-LFP porous microsphere that remained 72% of the initial capacity at 10 C. The graphene oxide-Li_3PO_4 (GO-LP) porous microsphere was prepared firstly by a facile precipitation method. Then GO-LP reacted hydrothermally with $FeSO_4$ to prepare G-LFP porous microspheres. G-LFP exhibits better electrochemical performance than $LiFePO_4$.

2. EXPERIMENTAL

2.1. Synthesis procedure

Graphite oxides were prepared from natural graphite flakes by a modified Hummers Method [15]. The GO-LP was prepared by a facile precipitation method. Typically, 50 mg GO was dispersed thoroughly by ultrasonic in 50 ml of water, and mixed with 1.1529 g H_3PO_4 (85%) under violent stirring. Then LiOH solution (50 ml 0.6 M, fresh prepared) was added to the mixture to produce GO-LP. The brown solution turned to gray and muddy. As soon as the reaction was finished, the precipitate was filtered and washed with deionized water and ethanol three times, respectively, and dried at 60 ℃ overnight. The obtained sample was used for the preparation of G-LFP composite. The as prepared GO-LP, $FeSO_4$ and glucose (20 wt. %) were mixed in water under a nitrogen atmosphere. The molar ratio of Li:Fe:P was 3:1:1. Keeping vigorous stirring for a few minutes, the suspension was then transferred to a 50 ml Teflon autoclave and kept at 200 ℃ for 10 h. After reaction, the obtained precipitate was washed with sufficient water and dried at 60 ℃ in vacuum overnight. Then the G-LFP was annealed at 600 ℃ for 5 h under 5% H_2/Ar atmosphere. The heating rate was 5 ℃ min^{-1}.

The $LiFePO_4$ sample was synthesized under the same condition using Li_3PO_4 as reactant for comparison.

2.2. Structural and morphological characterization

The prepared samples were characterized by field-emission scanning electron microscopy (SEM, Hitachi S-4800) and high resolution transmission electron microscopy (HRTEM, JEOL-2100). The crystalline structures of the samples were identified by an X-ray diffractometer (Bruker D8 Advance X-ray diffraction). N_2 adsorption was performed at -196 ℃ in a Quadrasorb SI system.

Raman spectra were recorded on a LabRAM HR800 Raman microprobe (HORIBA JY) with 632 nm laser excitation.

2.3. Electrochemical characterization

Electrochemical performances of samples were investigated with a CR2016 coin cell composed of the cathode, lithium anode, a Celgard polypropylene separator, and $LiPF_6$ in 1:1 ethylene carbonate (EC) and diethyl carbonate (DEC) as the electrolyte. The cathode was prepared by a slurry coating process. The slurry, obtained by mixing the active materials, acetylene black and polyvinylidene fluoride (PVDF) at a weight ratio of 80:10:10 in N-methylpyrrolidinone, was uniformly pasted onto Al foils and dried in vacuum, with a typical material loading of 3 mg cm^{-2}. All cells were fabricated in an argon-filled glove box. The charge/discharge measurements were carried out with Neware test system within a voltage range from 2.0 to 4.2 V vs. Li^+/Li at room temperature.

3. RESULTS AND DISCUSSION

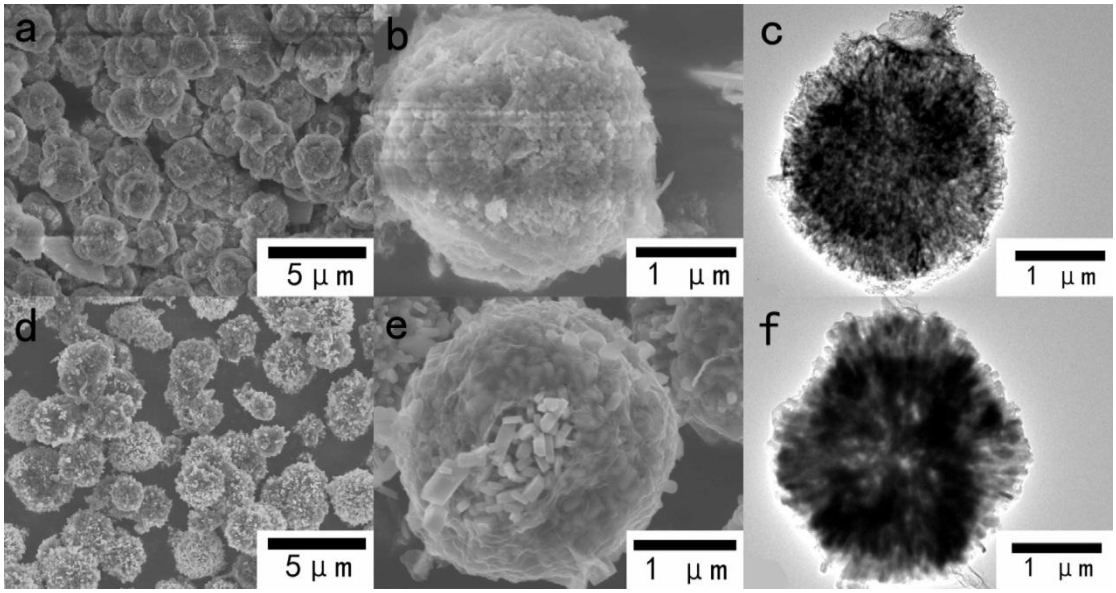

Figure 1. SEM images of GO-LP (a, b) and G-LFP (d, e); TEM images of GO-LP (c) and G-LFP (f).

As shown in Fig. 1a, GO-LP exhibits a microsphere shape with about 2 μm in diameter. And GO nanosheets wrapped on LP microspheres can be seen clearly (Fig. 1b). From the TEM image (Fig. 1c), the porous microspheres are comprised of nanoparticles. G-LFP has the similar morphology. The average particle size of G-LFP microspheres is around 2 μm (Fig. 1d). The microspheres constituted by about 200 nm particles were covered by the graphene nanosheets (Fig. 1e). And the porous structure can also be seen in Fig. 1f. Because of the different K_{sp} (solubility product) between Li_3PO_4 and

$Fe_3(PO_4)_2$, the Li_3PO_4 microsphere played a role as a sacrificial template during the hydrothermal reaction, leading to the porous spherical structure of $LiFePO_4$ [16].

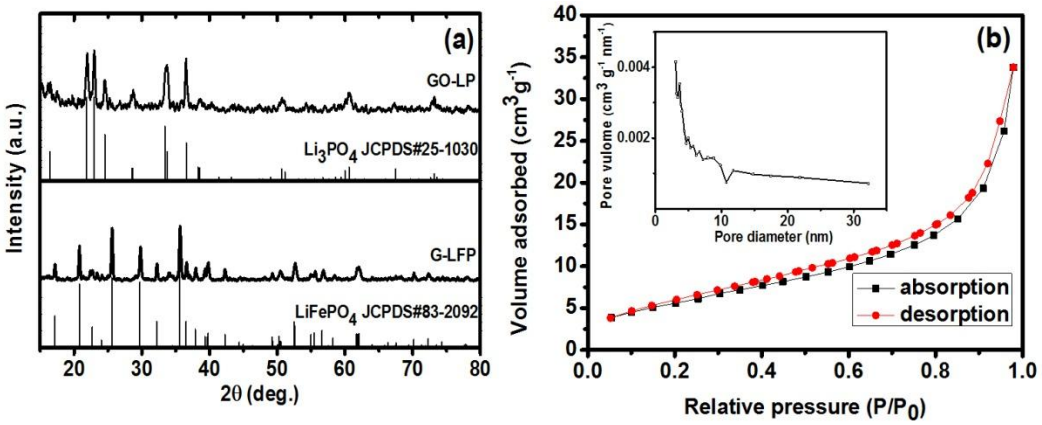

Figure 2. X-ray diffraction (XRD) patterns of GO-LP and G-LFP (a); Nitrogen adsorption and desorption isotherms of G-LFP (b). The inset is their pore-size distributions.

The crystal structures of as-prepared GO-LP and G-LFP were determined by X-ray diffraction (XRD) spectrometry. As shown in Fig. 2a, all diffraction peaks could be indexed to the orthorhombic Li_3PO_4 (JCPDS#25-1030) and $LiFePO_4$ (JCPDS#83-2092), respectively. No impurity can be found.

The adsorption-desorption isotherm for G-LFP appears to be a type IV isotherm with an H3 hysteresis loop(Fig. 2b), indicating a porous characteristic which is aggregates of plate-like particles giving rise to slit-shaped pores [17]. The measured Brunauer-Emmett-Teller (BET) area for G-LFP is 21.017 m^2 g^{-1}. The average pore diameters and the corresponding BJH desorption cumulative pore volumes are 3.414 nm and 0.047 cm^3 g^{-1}, respectively.

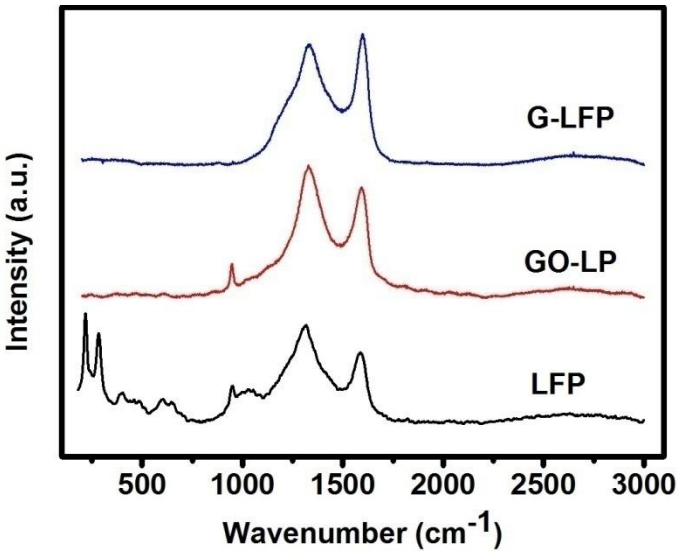

Figure 3. Raman spectra of the samples: $LiFePO_4$, GO-LP and G-LFP.

Raman spectra of composites were taken to verify the reduction of graphene in the samples and explored the surface properties of the samples (Fig. 3). The samples exhibit characteristic Raman peaks of carbon at around 1330 and 1595 cm^{-1}, which are attributed to the D band (disordered carbon, sp^3) and the G band (ordered graphitic carbon, sp^2) of Raman vibration modes for carbon, respectively [18]. Full width at half maximum (FWHM) of the G band for G-LFP (84.1 cm^{-1}) is smaller than that for GO-LP (116.7 cm^{-1}), and the intensity ratio of the D peak to the G peak (I_D/I_G) of G-LFP (0.92) is reduced compared with that of GO-LP (1.19). Both of changes suggest that graphene oxide have been reduced to graphene [19]. Meanwhile, the intensity of the G peak and D peak for $LiFePO_4$ are weak, due to its low content of carbon. And the peaks that wavenumber less than 1100 cm^{-1} are assigned to the fingerprint peaks of orthorhombic symmetry $LiFePO_4$ [20]. However, for G-LFP, even no Raman signals can be distinguished in this range compared with $LiFePO_4$, because graphene coated on the microspheres screen the Raman signals of $LiFePO_4$ [21].

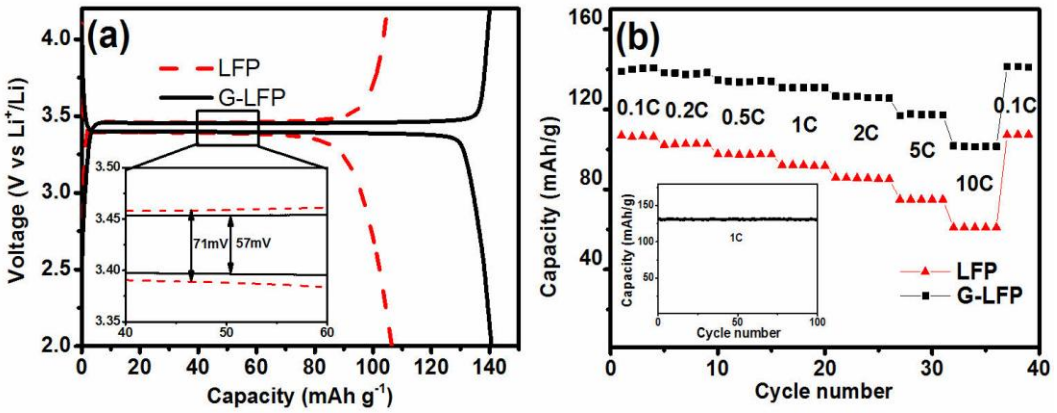

Figure 4. Charge and discharge profiles vs. lithium at a current rate of 0.1 C for G-LFP and $LiFePO_4$ (a), the inset shows the flat regions magnified; and rate performance of G-LFP (■) and $LiFePO_4$ (▲) (b), the inset show discharge capacities during continuous cycling of G-LFP at 1 C.

The initial charge/discharge potential profiles obtained from $LiFePO_4$ and G-LFP cells at 0.1 C are shown in Fig. 4a. For the G-LFP electrode, the initial charge/discharge capacity at 0.1 C is 141 mAh g^{-1}. It is higher than that of $LiFePO_4$ (106 mAh g^{-1}). In the inset of Fig. 4a, the voltage difference between the plateaus of the charge/discharge curves for G-LFP is smaller (57 mV at 0.1 C) than that of $LiFePO_4$ (71 mV at 0.1 C), which indicates G-LFP have superior electrochemical kinetics properties. The more remarkable advantage of G-LFP is on the aspects of the rate performance. In Fig. 4b, discharge capacities of the G-LFP measured at various rates are130.9 mAh g^{-1} at 1 C and 101.8 mAh g^{-1} at 10 C, while there is only 61 mAh g^{-1} at 10 C for $LiFePO_4$. When the current rate goes back to 0.1 C after cycling at high rate, the cell capacity can almost recover to the original value, which indicates that the sample owns good stability. The good stability is also showed in the inset of Fig. 4b, that the discharge capacity of G-LFP did not fade after 100 cycles at 1 C. The good electrochemical performance of G-LFP is attributed to two reasons. One is the enhanced conductive samples, due to the

high conductive graphene coated on $LiFePO_4$ and the unique two-dimensional planar structure that graphene nanosheets showed plane-to-point electric contact with $LiFePO_4$ particles [22]. The other is the porous structure of $LiFePO_4$, which can make the electrolyte infuse the interior of sample to decrease the distance of lithium ion diffusion.

4. CONCLUSIONS

In summary, we have synthesized GO-LP by a precipitation method, and used it as sacrificial template to prepare G-LFP composites by hydrothermal treatment. The morphology of G-LFP was microsphere wrapped by graphene nanosheets. And the microspheres were assembled from tiny nanoparticles. The cathodes made from G-LFP delivered excellent discharge capacities of 141, 130.9 and 101.8 mAh g^{-1} at current rates of 0.1 C, 1 C and 10 C, respectively, due to the effective conducing network formed by bridging graphene nanosheets and the porous structure which could absorb the electrolyte to help lithium ion to diffusion. The way, which uses GO-LP or similar phosphate composite (GO-$Fe_3(PO_4)_2$, GO-$MnPO_4$) as raw material, shows the potential to synthesize graphene-phosphate composite, such as graphene-$LiFePO_4$, graphene-$LiMnPO_4$ or graphene-$LiCoPO_4$.

ACKNOWLEDGEMENTS
This work was supported by National Basic Research Program of China (2009CB930503), NSFC (Contract No.50823009), the Fund for the Natural Science of Shandong Province (ZR2010EM020, ZR2010EM049), the Scientific Development Planning of Shandong Province (2010GGX10340) and IIFSDU (2012JC007)

References

1. A.K. Padhi, K.S. Nanjundaswamy, C. Masquelier, S. Okada, J.B. Goodenough, *J. Electrochem. Soc.*, 144 (1997) 1609.
2. S.F. Yang, Y. Song, P.Y. Zavalij, M.S. Whittingham, *Electrochem. Commun.*, 4 (2002) 239.
3. A. Yamada, S.C. Chung, K.J. Hinokuma, *J. Electrochem. Soc.*, 148 (2001) A224.
4. A.K. Padhi, K.S. Nanjundaswamy, J.B. Goodenough, *J. Electrochem. Soc.*, 144 (1997) 1188.
5. H. Huang, S.C. Yin, L.F. Nazar, *Electrochem. Solid-State Lett.*, 4 (2001) A170.
6. P.P. Prosini, M. Carewska, S. Scaccia, P. Wisniewski, M. Pasquali, *Electrochim. Acta*, 48 (2003) 4205.
7. A. Magasinski, P. Dixon, B. Hertzberg, A. Kvit, J. Ayala, G. Yushin, *Nat. Mater.*, 9 (2010) 353–358.
8. K.S. Novoselov, A.K. Geim, S.V. Morozov, D. Jiang, Y. Zhang, S.V. Dubonos, I.V. Grigorieva, A.A. Firsov, *Science*, 306 (2004) 666.
9. L. Wang, H.B. Wang, Z.H. Liu, C. Xiao, S.M. Dong, P.X. Han, Z.Y. Zhang, X.Y. Zhang, C.F. Bi, G.L. Cui, *Solid State Ionics*, 181 (2010) 1685.
10. Y. Zhang, W.C. Wang, P.H. Li, Y.B. Fu, X.H. Ma, *J. Power Sources*, 210 (2012) 47.
11. J.L. Yang, J.J. Wang, D.N. Wang, X.F. Li, D.S. Geng, G.X. Liang, M. Gauthier, R.Y Li, X.L. Sun, *J. Power Sources*, 208 (2012) 340.
12. Y. Wang, Z.S. Feng, J.J. Chen, C. Zhang, *Mate. Lett.*, 71 (2012) 54.
13. Y. Ding, Y. Jiang, F. Xua, J. Yin, H. Ren, Q. Zhuo, Z. Long, P. Zhang, *Electrochem. Commun.*, 12

(2010) 10.
14. A. Magasinski, P. Dixon, B. Hertzberg, A. Kvit, J. Ayala, G. Yushin, *Nat. Mater.*, 9 (2010) 353.
15. S.H. Aboutalebi, M.M. Gudarzi, Q.B. Zheng, J.K. Kim, *Adv. Funct. Mater.*, 21 (2011) 2978.
16. M.H. Lee, J.Y. Kim, H.K. Song, *Chem. Commun.*, 46 (2010) 6795.
17. K.S.W. Sing, D.H. Everett, R.A.W. Haul, L. Moscou, R.A. Pierotti, T. Siemieinewska, *Pure Appl. Chem.*, 57 (1985) 603.
18. A.C. Ferrari, J. Robertson, *Phys. Rev. B*, 61 (2000) 14095.
19. A. Jorio, E.H.M. Ferreira, M.V.O. Moutinho, F. Stavale, C. Achete, R.B. Capaz, *Phys. Status Solidi B*, 247 (2010) 2980.
20. A.A. Salah, A. Mauger, K. Zaghib, *J. Electrochem. Soc.*, 153 (2006) A1692.
21. C.M. Julien, K. Zaghib, A. Mauger, M. Massot, A. Ait-Salah, M. Selmane, F. Gendron, *J. Appl. Phys.*, 100 (2006) 063511.
22. X.L. Li, Y.L. Zhang, H.F. Song, K. Du, H. Wang, H.Y. Li, J.M. Huang, *Int. J. Electrochem. Sci.*, 7 (2012) 7111